Available online at www.sciencedirect.com
SCIENCE DIRECT®
Journal of the European Ceramic Society 25 (2005) 3605–3610
www.elsevier.com/locate/jeurceramsoc

Synthesis and thermal expansion of ZrO_2/ZrW_2O_8 composites

P. Lommens, C. De Meyer, E. Bruneel, K. De Buysser*, I. Van Driessche, S. Hoste

Department of Inorganic and Physical Chemistry, Ghent University, Krijgslaan 281, Bld. S3, 9000 Ghent, Belgium

Received 10 July 2004; received in revised form 19 September 2004; accepted 24 September 2004
Available online 8 December 2004

Abstract

In this work, a ceramic composite of ZrW_2O_8 and ZrO_2 was synthesized, in order to investigate the possibility of compensating the positive thermal expansion of ZrO_2 with the negative thermal expansion (NTE) compound ZrW_2O_8, tailoring the thermal expansion of these composites. The NTE material was mixed with varying amounts of ZrO_2. The thermal expansion coefficients of this series of composites decrease with increasing amounts of ZrW_2O_8. Nevertheless, a negative deviation from the values expected by the rule of mixtures was found to be most pronounced in the middle of the compositional region.

Keywords: Sintering; Composites; Thermal expansion; ZrW_2O_8; X-ray methods; ZrO_2

1. Introduction

Most materials expand on heating and thus have a positive thermal expansion. Nevertheless, in recent years several families of materials with a negative thermal expansion (NTE) have been discovered. The ceramic material ZrW_2O_8 is one of the best known. This cubic material has an exceptionally large and isotropic negative thermal expansion over its entire stability range (−273 to 770 °C). The dimensions of this cubic material decrease linearly with temperature and at about 150 °C a phase transition from α-ZrW_2O_8 to β-ZrW_2O_8 can be observed.[1–3] A broad range of applications have been suggested for these NTE materials. One of the most obvious is the use in composites where the thermal expansion coefficient of the bulk material can be tailored to a specific value by combining a NTE material with a positive thermal expansion material. This may result in new materials with precisely matched expansion, being positive, negative or even zero, by adjusting the volume fraction of the different phases. These controlled expansion composites can be used in high precision optical mirrors, fibre optic systems, electronic devices or as a thermal package for fibre Bragg gratings. Although many applications were proposed for these new materials, the published research literature on this subject is still very limited. Only the Cu/ZrW_2O_8 composite has been more thoroughly studied.[4–6] This combination was chosen for its possible high thermal and electrical conductivity. Preliminary studies of cement/ZrW_2O_8 composites yielding zero expansion mortars[7] and Al/ZrW_2O_8[8] composites have been published.

In this work, the microstructure and thermo-mechanical properties of a two-phase ceramic composite consisting of ZrW_2O_8 and ZrO_2 are studied, with special emphasis on the coefficients of thermal expansion for different compositions ranging from 0 to 100 vol.% of ZrW_2O_8. Furthermore, the synthesis of the composites will be discussed, including an optimized preparation of ZrW_2O_8 based on our earlier published spray drying technique.[9]

2. Experimental

2.1. Synthesis of the composites

The starting materials consisted of a commercial ZrO_2 powder (Aldrich) and ZrW_2O_8 prepared using the spray drying technique. The synthesis of ZrW_2O_8 involves sev-

* Corresponding author.
E-mail address: klaartje.debuysser@rug.ac.be (K. De Buysser).

0955-2219/$ – see front matter © 2004 Elsevier Ltd. All rights reserved.
doi:10.1016/j.jeurceramsoc.2004.09.015

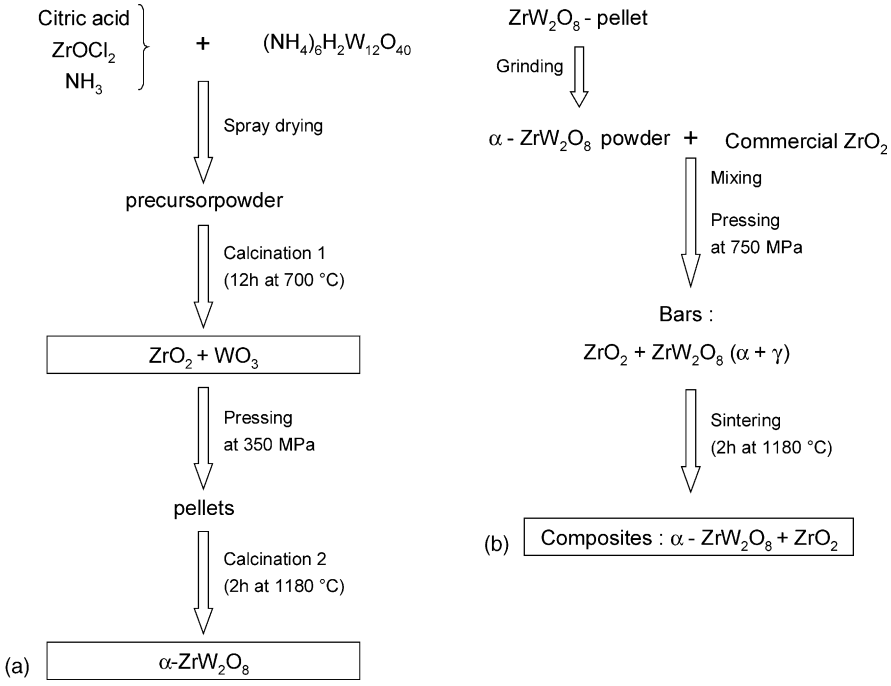

Fig. 1. Synthesis scheme for (a) ZrW_2O_8 via the spray drying technique and (b) preparation of the ZrW_2O_8/ZrO_2 composites.

eral successive steps as summarized in Fig. 1a. An aqueous precursor solution was prepared starting from ammonium metatungstate, $(NH_4)_6H_2W_{12}O_{40}\cdot nH_2O$ (Aldrich), zirconium oxychloride, $ZrOCl_2\cdot nH_2O$ (Aldrich) and citric acid, as a complexing agent to prevent hydrolysis and precipitation of the salts.[9] The 100 ml 0.042 M W-salt solution was slowly added to 100 ml of a solution containing 0.25 M Zr-solution and 0.25 M citric acid. NH_3 was used to raise the pH of the Zr-solution from 0.3 to 6. This transparent, colourless solution was then spray-dried using a Büchi 190 mini spray dryer with a 0.5 mm nozzle and a feeding rate of 5 ml per minute at temperatures close to 250 °C. This spray-dried powder was subsequently calcined at 700 °C for 12 h to yield an intimate mixture of ZrO_2 and WO_3. After calcination, these powders were uni-axially, cold pressed in pellets (250 mm Ø × 1 mm) at a pressure of 350 MPa. After heating in a covered Pt crucible at 1180 °C in a preheated furnace under air during 2 h, the pellets were quenched in liquid nitrogen, to prevent decomposition of the formed ZrW_2O_8 phase into ZrO_2 and WO_3.

For the preparation of the composites, the above pellets were ground in a mortar and manually mixed with different amounts of ZrO_2 (Fig. 1b). The properties of these powders are summarised in Table 1. The mixture was then uni-axial, cold pressed into bars (2 mm × 2 mm × 13 mm) at a pressure of 750 MPa. The bars were sintered at 1180 °C for 2 h under air in a covered Pt crucible, again in a preheated furnace and subsequently quenched in liquid nitrogen. A bar of pure ZrO_2 was prepared, using the same conditions.

Table 1
Powder specifications

Material	Particle size, d_{50} (μm)	d_{90} (μm)
ZrW_2O_8	12.77	32.46
ZrO_2 (Aldrich)	5.27	8.72

For all prepared materials, the mass differences between the green and sintered bodies were found to fall between 1 and 2%. This indicates that, even if there is a possible contribution of the volatilization of tungsten oxide to the mass loss during the thermal treatment, the effect of it is very limited and constant.

2.2. Experimental techniques

Particle size and particle size distribution of the different powders dispersed in de-ionized water were determined by laser diffraction (Malvern Particle Sizer Series 2600c). The geometrical density of the samples was measured. The microstructures of the polished cross-sections and fracture surfaces were observed by optical microscopy (Leitz labolux 12 pol S), scanning electron microscopy and EDX (Philips 501). Identification of the different phases present in the samples was performed by XRD analysis (Siemens D5000 diffractometer) using Cu Kα radiation on ground samples. The quantitative phase composition was estimated by whole pattern quantitative analysis of the X-ray diffraction patterns using the program FULLPROF.[10] The coefficients of thermal expansion were measured with a vertical push rod thermomechanical analyzer (TA Instruments) 2940, using a heating rate of 2 °C per minute from room temperature to 300 °C under a constant compressive force of 0.5 N, low enough to prevent deformation of the bars.

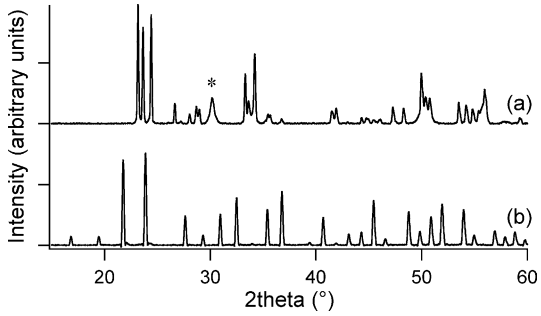

Fig. 2. X-ray diffraction pattern of (a) ZrO_2 and WO_3 mixture obtained after 12 h calcination at 700 °C of the spray-dried precursor powder, asterisk (*) indicates the reflection most characteristic for ZrO_2, and (b) α-ZrW_2O_8 powder after 2 h calcining at 1180 °C.

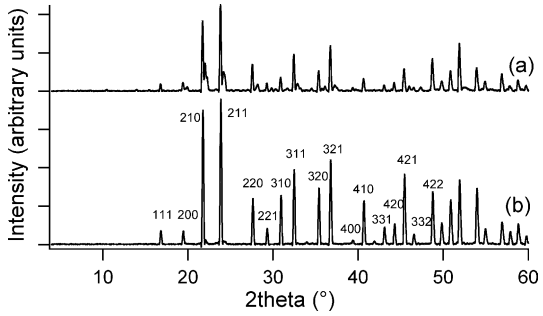

Fig. 3. X-ray diffraction pattern from (a) α + γ-ZrW_2O_8 mixture after pressing, and (b) a pure α-ZrW_2O_8 phase.

3. Results and discussion

3.1. Zirconium tungstate composites using the spray drying technique

Spray drying of the precursor solution yielded 60% of the total initial mass of the used starting salts. After calcination at 700 °C during 12 h, a stoichiometric mixture of ZrO_2 and WO_3 was formed (Fig. 2a) with an average particle size of 4.27 μm and a pycnometric density of 6.55 g/cm^3, which is in good agreement with the expected theoretical density of 6.84 g/cm^3 for a 1:2 molar ratio mixture of ZrO_2 (5.85 g/cm^3) and WO_3 (7.16 g/cm^3), respectively. The crystalline product obtained after thermal treatment at 1180 °C shows X-ray diffraction reflections of only cubic α-ZrW_2O_8 (Fig. 2b). The ZrW_2O_8 powder obtained by manually milling these pellets had an average particle size of 12.77 μm, Table 1.

Samples with a composition, ranging from 0 to 100 vol.% ZrW_2O_8, were prepared by manually mixing varying amounts of synthesized ZrW_2O_8 and commercial ZrO_2 and pressing these powder mixtures into bars.

3.2. Analysis of a pressed, pure ZrW_2O_8 sample

X-ray diffraction analysis of a pure (100 vol.%), ground, zirconium tungstate bar after pressing, showed that the pressure used for uni-axial pressing of the bars (750 MPa) was sufficiently high to drive a phase transition from cubic α-ZrW_2O_8 ($\rho = 5.081$ g/cm^3) to the high pressure phase, orthorombic γ-ZrW_2O_8 ($\rho = 5.375$ g/cm^3), see Fig. 3. This is reflected in the thermal expansion data of this bar, containing approximately 20 vol.% γ-ZrW_2O_8 and 80 vol.% α-ZrW_2O_8 (Fig. 4a). An expansion curve of cubic α-ZrW_2O_8 has been included for reference (Fig. 4b). Experimental thermal expansion coefficients obtained from this experiment are listed in Table 2. γ-ZrW_2O_8 is known to possess a negative coefficient of thermal expansion (-1.0×10^{-6} °C^{-1}) which is almost an order of magnitude less than for α-ZrW_2O_8 (-9.07×10^{-6} °C^{-1} from 0 to 100 °C).[1] It reverts to the cubic form by heating to 120 °C, accompanied by a volume

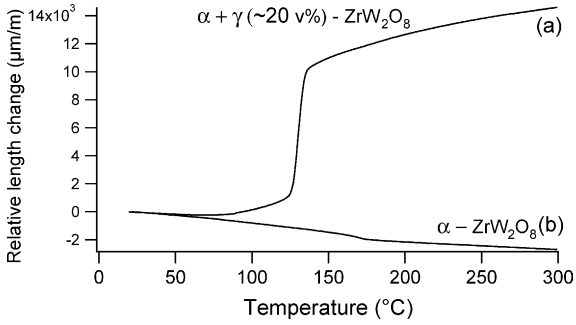

Fig. 4. Thermal expansion curve of (a) a pressed bar containing the α + γ-ZrW_2O_8 mixture and (b) a bar containing pure α-ZrW_2O_8. The plot shows the relative change in length from 25 to 300 °C.

expansion of 5 vol.%. As was expected, the high pressure sample shows negative thermal expansion behaviour below 100 °C. A large volume expansion can be seen between 100 and 150 °C, due to the γ to α transition. After this transition, the thermal expansion of this bar is, unexpectedly, still positive indicating that the transition to the low pressure phase is still ongoing. The behaviour depicted in Fig. 4 suggests the existence of two different regimes of dimensional change: (1) a fraction of the γ-phase is free to undergo the γ to α transition in an unconstrained manner, which corresponds to the large step at 120 °C and (2) a second fraction may be partially encapsulated and become subjected to such mechanical stresses that a different structural behaviour ensues and this is responsible for the tailing of the curve above 120 °C. Consider the high pressure phase surrounded by a majority of shrinking cubic ZrW_2O_8 as in Fig. 5a. Heating the bar to 120 °C starts the transition of the high pressure phase to the less dense cubic low pressure phase which is associated

Table 2
Experimental thermal expansion coefficients derived from the dilatometry data showed in Fig. 3

Sample	Thermal expansion coefficient ($\times 10^{-6}$ °C^{-1})	Temperature range (°C)
(a) Bar pressed at 750 MPa	−4.30	0–75
(a) Bar pressed at 750 MPa	23.45	150–300
(b) α-ZrW_2O_8	−12.11	0–150
(b) β-ZrW_2O_8	−6.32	200–300

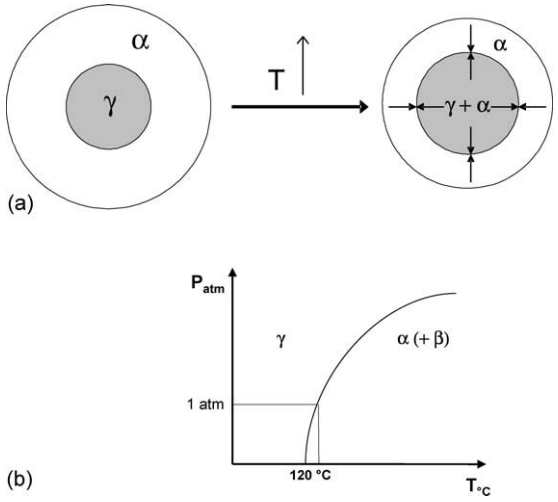

Fig. 5. (a) Illustration of the thermal stresses arising from the presence of γ-ZrW_2O_8 and (b) schematic representation of the phase diagram as suspected from our data for the the α to γ-ZrW_2O_8 transition.

with a large volume expansion while the surrounding cubic fraction is contracting. This gives rises to very large thermal stresses, high enough to prevent the complete transition of the orthorhombic high pressure to the cubic low pressure phase. One could say, the thermal stresses cause a shift of the γ to α transition to higher temperatures as presented in the phase diagram proposed in Fig. 5b. Upon cooling, the normal thermal expansion coefficients were again measured, proving the reversibility of the phenomenon. Finally, it is important to note that the γ-phase does not occur in the composites because it is completely transformed to β-phase during subsequent sintering at 1180 °C.

3.3. Analysis of the ZrW_2O_8/ZrO_2 composites

After sintering the respective mixtures containing different molar ratios of zirconium tungstate/zirconium oxide for 2 h at 1180 °C and subsequent quenching, the bars retained their original shape and did not show visible cracks. This indicates that these bars are able to withstand the thermal stresses created during heating and quenching remarkably well. These stresses originate from the large thermal volume expansion accompanying the gamma to alpha zirconium tungstate transition as shown before, in addition to the differences in thermal expansion coefficient between ZrW_2O_8 ($-9.1 \times 10^{-6}\,°C^{-1}$ from 0 to 100 °C and $-5.4 \times 10^{-6}\,°C^{-1}$ from 200 to 350 °C) and ZrO_2 ($9.6 \times 10^{-6}\,°C^{-1}$).

X-ray diffraction analysis confirms that only α-ZrW_2O_8 and monoclinic ZrO_2 are present, as shown for a 50 vol.% ZrW_2O_8 sample in Fig. 6. No high pressure γ-ZrW_2O_8 was found.

The geometrical densities of the green and sintered composite bars were measured. The theoretical density for the different bars was calculated from the theoretical values for ZrW_2O_8 (5.08 g/cm^3) and ZrO_2 (5.83 g/cm^3) and compared to the experimental geometrical densities. The obtained results are graphically shown in Fig. 7. Each data point presents the results of one or two bars. For the composite with the highest ZrW_2O_8 content, the sintering treatment results in a reduction of the porosity of the bars. For the compositions of 50%:50% ZrO_2:ZrW_2O_8 and those with lower concentrations of ZrW_2O_8, the sintering treatment doesn't result in a further reduction of the porosity. The final density equals the initial green density of the composite bars. This is also reflected in their microstructures (Fig. 8). The pure ZrW_2O_8 sample is micro-structurally very different from the 50 vol.% composite. As ZrO_2 sinters at much higher temperatures than ZrW_2O_8 (2100 °C), only the latter phase is sintered during the heating step at 1180 °C and the ZrO_2-phase remains as loose powder between the larger ZrW_2O_8 grains. Furthermore, its presence hinders the sintering of the ZrW_2O_8 phase. This assumption was confirmed by closer investigation of the microstructures presented in Fig. 8. EDX-mapping of Fig. 8d showed that the sintered, homogene areas, indicated with an asterisk (*) contain Zr and W atoms while in the area consisting of non-sintered grains, indicated with a (°), predominantly Zr atoms were found.

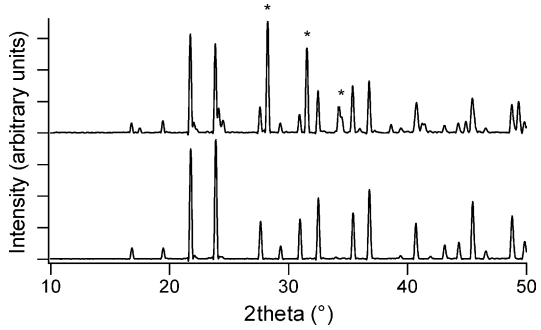

Fig. 6. X-ray diffraction pattern from the (a) 50 vol.% ZrW_2O_8/ZrO_2 mixture after sintering, asterisk (*) indicate the most characteristic reflections for monoclinic ZrO_2 and (b) pure α-ZrW_2O_8.

3.4. Thermal expansion of the composites

As can be expected, the thermal expansion coefficient of the composite decreases, when the zirconium tungstate to zirconium oxide ratio increases. In Fig. 9 the thermal expansion coefficients calculated from the rule of mixtures ($\alpha_c = \Sigma\alpha_i V_i$)

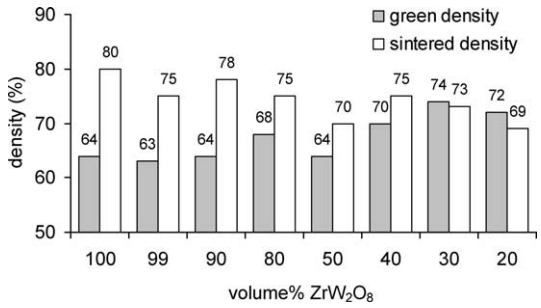

Fig. 7. Geometrical density of green and sintered composite bars in function of the composition.

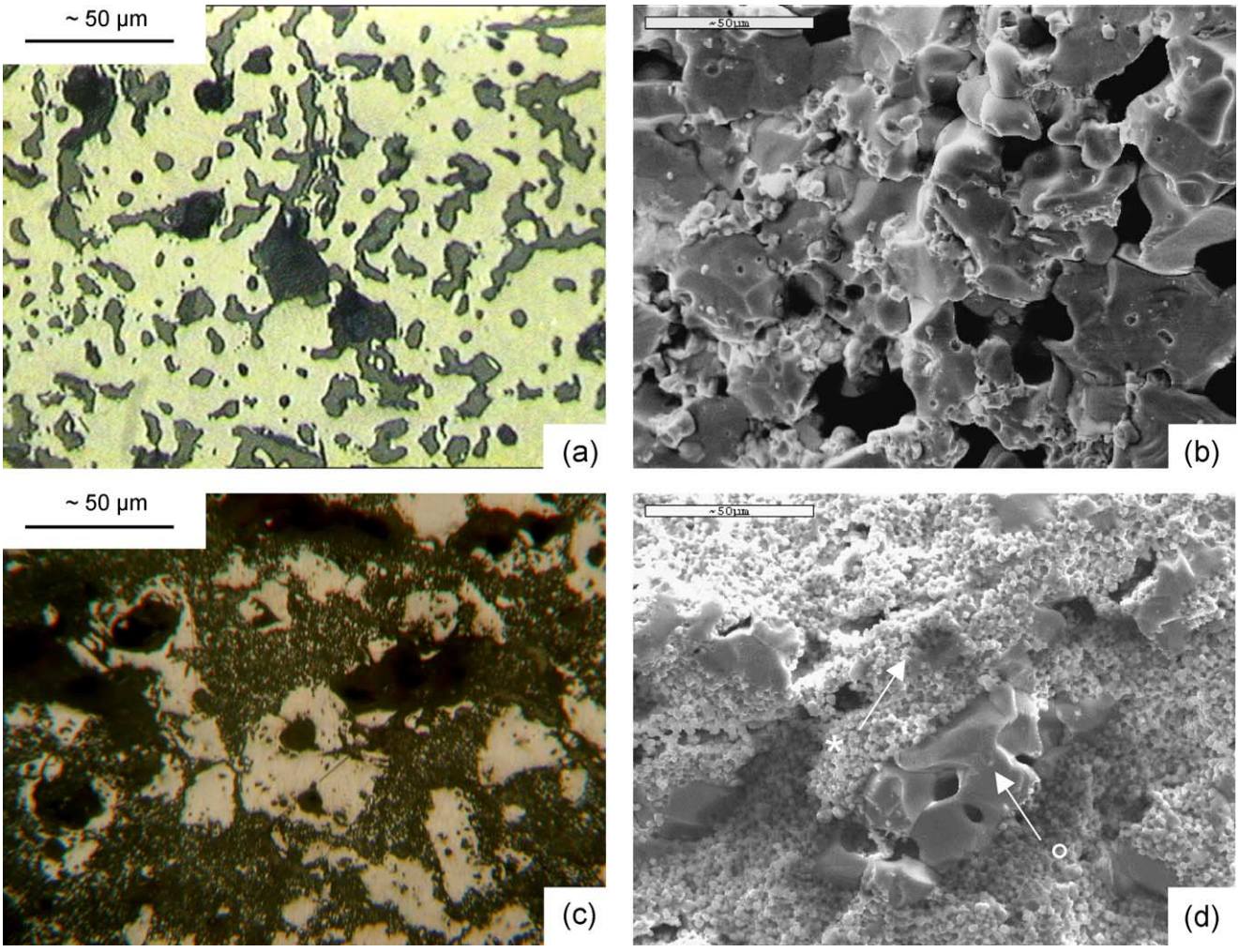

Fig. 8. (a) Optical micrograph of a polished cross-section and (b) a scanning electron micrograph of a fracture surface, both from a 100 vol.% ZrW_2O_8 sample, (c) optical micrograph of a polished cross-section and (d) SEM view of a fracture surface, both from a 50 vol.% composite.

at 225 °C are compared to the experimental data. The greatest deviation is found in the middle of the compositional range, which can be explained as follows: the rule of mixtures is only valid for a sample without voids, free of thermal stresses and when the different phases have the same elastic modulus.[11,12] Here, none of these conditions is fulfilled. Clearly in the middle of the compositional region, where the differences in thermal expansion coefficient and elastic modulus cause the highest stresses, the thermal expansion coefficient deviates the most from the expected coefficient. Using the rule of mixtures, the value of the thermal expansion coefficient was predicted to remain negative down to a volume ratio of 55 vol.% (at 225 °C). However, we found that volume ratios well below 55% still yielded negative expansion. This may have important technological consequences because it shows that a relatively low volume fraction of ZrW_2O_8 is sufficient to compensate effects of thermal expansion in a powderous matrix. This negative deviation relative to the rule of mixtures was found in many other composite systems.[12] This can be attributed to effects related to porosity, differences in elastic moduli and the incomplete sintering of these composites.

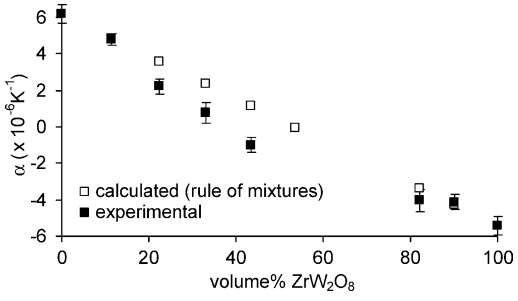

Fig. 9. Thermal expansion coefficients, calculated and experimental, at 498 K. The presented experimental coefficients are the weighed averages of the data for three samples.

4. Conclusion

This study demonstrates the possibility of synthesizing ceramic composites with a tailored thermal expansion

coefficient by introducing the NTE material ZrW_2O_8. ZrO_2/ZrW_2O_8 composites were synthesized that are able to withstand the thermal stresses, arising during sintering and subsequent quenching. The composites' coefficients of thermal expansion, measured between room temperature and 300 °C, decrease with increasing amounts of ZrW_2O_8. The coefficients of thermal expansion did not completely comply with the rule of mixtures since experimentally, lower volumes of ZrW_2O_8 were necessary to compensate for the positive thermal expansion of the ZrO_2 phase than those calculated using this rule.

Pressing the powder mixtures resulted in a partial transition of the α-ZrW_2O_8 into γ-ZrW_2O_8. This transition was still ongoing well above 120 °C, which was explained by considering the large thermal stresses originating from the α-phase encapsulating the γ-phase.

Acknowledgments

The authors would like to thank the Department of Solid State Physics at the University of Ghent for performing X-ray diffraction measurements and scanning electron microscopy. We would also like to thank R. Mouton for the technical support. Christy De Meyer is grateful for a Ph.D. grant by the fund of Scientific Research-Flanders (Belgium) (F.W.O.-Vlaanderen).

References

1. Mary, T. A., Evans, J. S. O., Vogt, T. V. and Sleight, A. W., Negative thermal expansion from 0.3 to 1050 kelvin in ZrW_2O_8. *Science*, 1996, **272**, 90–92.
2. Evans, J. S. O., Negative thermal expansion materials. *J. Chem. Soc. Dalton Trans.*, 1999, 3317–3326.
3. Sleight, A. W., Compounds that contract on heating. *Inorg. Chem.*, 1998, **37**, 2854–2860.
4. Verdon, C. and Dunand, D. C., High-temperature reactivity in the ZrW_2O_8-Cu system. *Acta Metall.*, 1997, **36**(9), 1075–1080.
5. Holzer, H. and Dunand, Phase transformation and thermal expansion of Cu/ZrW_2O_8 metal matrix composites. *J. Mater. Res.*, 1999, **14**(3), 780–789.
6. Yilmaz, S., Thermal mismatch stress development in Cu-ZrW_2O_8 composite investigated by synchrotron X-ray diffraction. *Comp. Sci. Technol.*, 2002, **62**, 1835–1839.
7. Kofteros, M., Rodriguez, S., Tandon, V. and Murr, L. E., A preliminary study of thermal expansion compensation in cement by ZrW_2O_8 additions. *Scripta Materialia*, 2001, **45**, 369–374.
8. Matsumoto, A., Kobayashi, K., Nishio, T. and Ozaki, K., Fabrication and thermal expansion of Al-ZrW_2O_8 composites by pulse current sintering. *Mater. Sci. Forum*, 2003, **426**(4), 2279–2283.
9. De Meyer, C., Van Driessche, I. and Hoste, S., Synthesis of the negative thermal expansion compound ZrW_2O_8 by the spray drying technique. *Key Eng. Mater.*, 2002, **11**, 206–213.
10. Rodriguez-Carvajal, S., FULLPROF: a program for Rietveld Refinement and Pattern Matching analysis. In *Abstracts of the Satellite Meeting on Powder Diffraction of the XV Congress of the IUCr*, 127. 1990.
11. Ho, Y., *Thermal Expansion of Solids*. ASM Int., 1998.
12. Chawla, K. K., *Ceramic Matrix Composites*. Chapman & Hall, London, 1993.